On the Delocalization of Electrons in Atoms and Molecules†

Robert L. Fulton‡

Department of Chemistry and Biochemistry, The Florida State University, Tallahassee, Florida 32306

Received: May 11, 2004; In Final Form: October 4, 2004

A quantitative measure of the delocalization of electrons from the region inside a sphere of radius R centered on a nucleus to the region exterior to this sphere is the atom delocalization index $\Delta(R)$. $\Delta(R)$ is defined by the double integral of the point−point sharing index $I(\zeta;\zeta')$ over two distinct volumes: ζ over the interior of a sphere of radius R, and ζ' over the remaining space. This index, as a function of R, has a remarkable shell-like structure with the values of the maxima being close to the number of electrons traditionally assigned to a particular shell times 0.25. The origin of these almost "magic" numbers and the reasons for deviations of these numbers from the simple rule is discussed in terms of simple models of the electronic structure of some light atoms. Results from numerical computations of electronic structure are presented for the atoms Li, Be, Al, Ne, Ar, Kr, Xe, Rn, Zn, and Au. The distinct shell-like structure of $\Delta(R)$ persists even to the heaviest of these. For atoms with zero total orbital angular momentum, the delocalization index can be split into a sum of noninterfering terms of different single particle angular momenta. These contributions also have distinctive shell-like structures. The maxima of the different angular momentum contributions do not always coincide. A similar decomposition also holds for spin "up" and "down" contributions. The shell-like structure allows for the identification of the spatial region in which the valence electrons lie. The angular momentum contributions can be used to identify the nature of the valence regions. The invariance of the core electron regions and the changes in the valence regions upon bond formation are illustrated by the calculation of the delocalization index for the heavy atoms in CH_4, NH_3, H_2O, and SiH_4. The identification of the spatial location of the valence regions should aid choosing the location of fixed points when analyzing the behavior of electrons using sharing amplitudes.

I. Introduction

The point−point sharing index $I(\zeta;\zeta')$ gives a quantitative measure of the degree to which a single electron in a many electron system is shared (delocalized) between two space-spin points ζ,ζ'.[1] (ζ stands for the three spatial indices together with a spin index.) This index obeys an important sum rule which allows for a consistent interpretation that scales properly with system size. The point−point sharing index is found from the underlying point−point sharing amplitude $\langle\zeta;\zeta'\rangle$, which itself is the matrix, positive semidefinite, square root of the single particle density matrix. The sharing amplitude is the closest possible analogue to a wave function for the description of a single electron in a many electron system. The sharing amplitude shares with a wave function the following properties: the amplitude may be complex; in general it has nodes; and, the absolute value squared of the amplitude gives the sharing index just as the absolute value squared of a normalized wave function gives the probability density.

Basin−basin sharing indices based on the double integration of the point−point sharing index over distinct atoms as defined by Bader[2] and basin−point sharing indices have been given for a number of molecules in previous papers.[3−5] These indices, in conjunction with sharing amplitudes, were used by Fulton and Perhacs[6] to analyze hydrogen bonding (and antibonding) in complexes formed from hydrides of the first row of eight elements in the periodic table. Because the sharing amplitude in general is a function of eight variables (six essential ones if the total spin of the wave function is zero), the amplitude is a more complex object to visualize than the basin−basin and basin−point sharing indices. To simplify the visualization of the amplitude, one point of the amplitude was fixed while the other point was initially left free to roam about three dimensions. Because the structure of the amplitude in the vicinity of the bridge proton was desired and because hydrogen, unique among the bonding atoms, has no electron core structure, the fixed point, e.g., ζ', was located on the bridge proton. The other point was then restricted to a two-dimensional surface so that the sharing amplitude in the region of the hydrogen bond could be characterized.

The question now arises as to the handling of the fixed points when dealing with atoms other than hydrogen. At a fixed point in the region in which the core electrons reside will give primarily the inner core structure of the atom. If we are to study the behavior of the electrons involved in the bonding in a molecule using sharing amplitudes, we need to determine the regions wherein the valence electrons reside and locate the fixed points in those regions. We should also like to have some quantitative indication that the sharing in the core region of an atom is essentially unaffected by the bonding of the atom to other atoms.

The suggestion of a referee of a previous paper provided additional motivation for this work, namely to check the sensitivity of the basin−basin sharing indices to the shapes and locations of the basin surfaces.

† Much of the material in this paper is contained in the Ph.D. dissertation of Petar M. Mitrasinovic done under the direction of the author. P. M. Mitrasinovic has not responded to repeated requests for his consent to be a coauthor, hence the lack of coauthorship.

‡ E-mail: fulton@chem.fsu.edu.

10.1021/jp0479825 CCC: $27.50
Published on Web 12/01/2004

In the next section we define the atom delocalization index $\Delta(R)$ as the quantitative measure of the sharing (delocalization) of an electron between the interior of a sphere of radius R centered on the nucleus of an atom and the volume exterior to that sphere. Some simplified models are considered to illustrate the almost magic numbers that appear; namely, the heights of the maxima of the delocalization index are approximately equal to the number of electrons in a shell, which are active in being shared across the spherical surface, times 0.25. Reasons for deviations from this simple rule are discussed. In addition, as a check on the number of electrons that are inactive in sharing across the spherical surface, the self-sharing index of the electrons within the spherical surface is considered.

This introduction is followed by a section in which the indices, based on calculated correlated wave functions, are presented for the atoms lithium, beryllium, aluminum, the rare gas atoms from neon through radon, and zinc and gold. For electronic states having a total orbital angular momentum of zero, the delocalization index can be decomposed into a sum of the contributions of single particle orbital angular momenta. These contributions are given for select atoms. In addition the spin up and spin down contributions are given for some atoms in nonsinglet spin states.

$\Delta(R)$, as a function of R, is found to have a rich shell structure with clear demarcations between the shells. The different shells correspond to the classic divisions of atomic electrons into, for example, 1s, 2s2p, 3s3p3d, etc., shells. Likewise, the contributions of the different single particle angular momenta to $\Delta(R)$, $\Delta_l(R)$ for angular momentum l, show a pronounced shell structure with the maximum values of $\Delta_l(R)$ again being closely related to the number of electrons having an angular momentum l which are active in that shell. These maxima, however, are not always at the same position in a given shell, this contributing to the discrepancy of the maximum from the naive counting given above. It is noted in conjunction with beryllium that, when correlation is included, there is a significant contribution of $l = 1$ to the delocalization index in the region of the second shell. The spin up and spin down contributions have behaviors similar to that found for the orbital angular momentum contributions.

The structure of the atom delocalization index therefore delineates not only the different shell regions of atoms but also the numbers of electrons actively shared between inner and outer portions of a given shell region together with the region in which the valence electrons reside.

The final section analyzes the atom delocalization index about the heavy atom in CH_4, in NH_3, in H_2O, and in SiH_4. In these we find that the delocalization index in the core region is virtually identical to that in the isolated atoms. The differences occur in the valence region. To illustrate the nonnegligible effects of correlation on the delocalization indices in the valence region, the results for methane, calculated at a correlated level, are compared to the results of a Hartree−Fock calculation.

II. Atom Delocalization Index

In this section, after a brief recall of the definitions of the sharing amplitude and point−point sharing index, we introduce the atom delocalization index $\Delta(R)$, which gives the sharing of an electron between the inner volume of a sphere of radius R centered on the nucleus and the outer volume. Following this we consider some very simple examples, the hydrogen atom, the helium atom, and the beryllium atom, to get a feel for some aspects of the delocalization index, including the origin of the pseudo "magic numbers" and the reasons these numbers are not precise. To complement the delocalization index, we also give the inner self-sharing index of beryllium, this giving the number of electrons within the sphere which are shared only to points within the sphere. In the special case of a total orbital angular momentum of zero, we note that the delocalization index can be written as a sum of independent contributions of the various single particle angular momenta.

Let ζ represent the three spatial coordinates $\boldsymbol{r}$ plus one spin coordinate σ

$$\zeta = (\boldsymbol{r}, \sigma) = (x, y, z, \sigma)$$

The point−point sharing index $I(\zeta;\zeta')$ is simply related to the sharing amplitude $\langle\zeta;\zeta'\rangle$ which in turn is found from the single particle density matrix $P(\zeta;\zeta')$, normalized such that the integral of $P(\zeta;\zeta)$ over all space and summed over spin is the total number N of electrons in the system. The relations are the following[1]

$$\langle\zeta;\zeta'\rangle = P^{1/2}(\zeta;\zeta')$$
$$I(\zeta;\zeta') = |\langle\zeta;\zeta'\rangle|^2$$

It is important to note that it is the positive semi-definite square root of the matrix and not the square root of the matrix element which is used in the connection between the sharing amplitude and the density matrix. One immediate consequence of these relations is the sum rule

$$\int \mathrm{d}\zeta'\, I(\zeta;\zeta') = P(\zeta;\zeta')$$

the quantity on the right being the electron density at the point ζ. It is this relation that gives consistency to the interpretation of the amplitudes and the indices. A second integral over ζ gives the total number of electrons in the system

$$\int \mathrm{d}\zeta\, \mathrm{d}\zeta'\, I(\zeta;\zeta') = N$$

In this paper we determine the sharing of an electron between the volume inside a sphere of radius R, centered on the nucleus of an atom, and the rest of the universe. The appropriate delocalization index $\Delta(R)$, the atom delocalization index, is defined as

$$\Delta(R) = \int_{|\boldsymbol{r}|\le R} \mathrm{d}\zeta \int_{|\boldsymbol{r}'|>R} \mathrm{d}\zeta'\, I(\zeta;\zeta')$$

the integrals over the variables implicitly including sums over the spin indices.

When expressed in terms of the natural spin−orbitals,[7] $\varphi_m(\zeta)$, the delocalization index is[8]

$$\Delta(R) = \sum_{m,n} \nu_m^{1/2} \nu_n^{1/2} (\varphi_m,\varphi_n)_{|\boldsymbol{r}|\le R} (\varphi_n,\varphi_m)_{|\boldsymbol{r}|>R} \qquad (1)$$

ν_m is the occupation number of the mth spin−orbital $\varphi_m(\zeta)$ and $(\varphi_m,\varphi_n)_{|\boldsymbol{r}|\le R}$ stands for the integral

$$(\varphi_n,\varphi_m)_{|\boldsymbol{r}|\le R} \equiv \int_{|\boldsymbol{r}|\le R} \mathrm{d}\zeta\, \varphi_m^*(\zeta)\, \varphi_n(\zeta)$$

$(\varphi_n,\varphi_m)_{|\boldsymbol{r}|>R}$ stands for a similar integral, but with the integration over the volume exterior to the sphere.

To illustrate the features of $\Delta(R)$ when applied to atoms, we consider several simplified models. The first is the electron in a hydrogen atom in the normalized pure state with "up" spin, $\varphi(\boldsymbol{r})\alpha(\sigma)$. The delocalization index in this case can be written in terms of the probability $p_{\mathrm{in}}(R)$ that the electron be found within the sphere as

$$\Delta(R) = p_{in}(R)\,[1 - p_{in}(R)]$$

$$p_{in}(R) = \int_{|\boldsymbol{r}|\le R} d\boldsymbol{r}\; \varphi^*(\boldsymbol{r})\,\varphi(\boldsymbol{r}) \qquad (2)$$

The maximum value of $\Delta(R)$ is 0.25, occurring at the radius for which the probability of finding the electron within the sphere is 0.50. If the wave function is nonvanishing at the nucleus, $\Delta(R)$ vanishes as the cube of the radius R as $R \rightarrow 0$:

$$\Delta(R) \approx \frac{4\pi}{3} R^3 |\varphi(0)|^2 \qquad (3)$$

When the state is the ground state of the electron in a hydrogen atom

$$\varphi(r) = \left(\frac{1}{\pi}\right)^{1/2} e^{-r} \qquad (4)$$

the probability of finding the electron within the sphere is

$$p_{in}(R) = 1 - e^{-2R}(1 + 2R + 2R^2)$$

The large R behavior of $\Delta(R)$ follows as

$$\Delta(R) \approx 2R^2 e^{-2R}$$

a power of R times an exponential which decreases with increasing size of the sphere. We expect this relatively slow exponential falloff with increasing radius to be a common asymptotic feature of the delocalization index. The small R behavior agrees with eq 3. Between these limits there is one maximum, found numerically to be at a radius of

$$R \approx 1.337$$

We note that this maximum occurs at a radius about one-third larger than the Bohr radius and less than the average radius of 1.5 for the 1s wave function. The radius scales inversely with the nuclear charge so that if the charge on the nucleus is Z, the radius at which the maximum occurs is

$$R \approx \frac{1.337}{Z}$$

The radial dependence of this delocalization index is given in Figure 1. The region in which the delocalization is largest is almost entirely localized within a distance of roughly 4 bohr from the nucleus. For example, the value of the delocalization index is 0.01 at a radius of 4.197, this giving an indication of the spatial extent of the region over which the electron is delocalized. The slow decrease of $\Delta(R)$ at values of R greater than 3 bohr as indicated above should be noted.

Because an integer times this maximum value of 0.25 tends to permeate (at least approximately) the numerical results of the next section, we consider some slightly more complicated models to show the origin of the factor and some reasons for discrepancies from this naive expectation. Consider a two electron atom in its ground singlet electronic state at the Hartree−Fock level approximation. Let $\varphi(\boldsymbol{r})$ be the spatial part of the Hartree−Fock orbitals. The delocalization index differs by a factor of 2 from eq 2

$$\Delta(R) = 2p_{in}(R)[1 - p_{in}(R)]$$

$$p_{in}(R) = \int_{|\boldsymbol{r}|\le R} d\boldsymbol{r}\; \varphi^*(\boldsymbol{r})\,\varphi(\boldsymbol{r})$$

The maximum of the delocalization index is now twice what it was in the case of the hydrogen atom, namely $2 \times 0.25 = 0.50$. If the spatial orbital is given by the hydrogen-like wave function (4) modified to have an effective nuclear charge of 1.6875 appropriate for the approximate ground state of He using this wave function, the maximum occurs at a radius of 0.792.

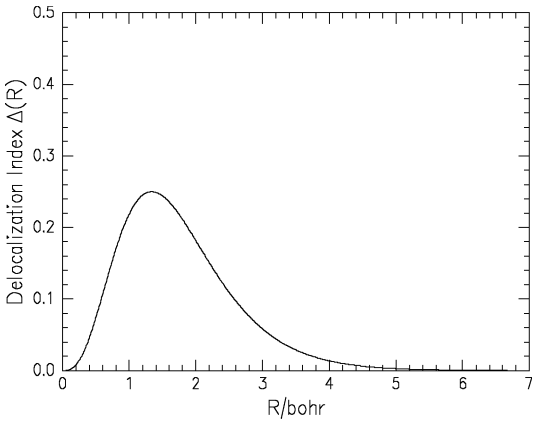

Figure 1. $\Delta(R)$ of a hydrogen atom.

Consider now the simplistic model of the electrons in the ground state of a beryllium atom given by a single determinant wave function. Let the spatial parts of the real orbitals used in forming the determinant be denoted by $\varphi_{1s}(r)$ and $\varphi_{2s}(r)$. The delocalization index is

$$\Delta(R) = 2[(\varphi_{1s},\varphi_{1s})_{|\boldsymbol{r}|\le R}(\varphi_{1s},\varphi_{1s})_{|\boldsymbol{r}|>R} + 2(\varphi_{1s},\varphi_{2s})_{|\boldsymbol{r}|\le R}(\varphi_{2s},\varphi_{1s})_{|\boldsymbol{r}|>R} + 2(\varphi_{2s},\varphi_{2s})_{|\boldsymbol{r}|\le R}(\varphi_{2s},\varphi_{2s})_{|\boldsymbol{r}|>R}] \qquad (5)$$

The first term on the right-hand side is a product of the probability that an electron assigned to a 1s orbital be found inside the sphere of radius R and the probability that it be found outside that sphere. The last term on the right-hand side is a similar product involving a 2s electron. If we consider the contributions of these terms separately, then each contributes 0.5 to their maximum, with the 2s maximum occurring at the larger of the two radii. When the terms are added, each maxima may be larger than 0.50 because, for example, the 2s contribution need not vanish at the position of the 1s maximum, hence increasing the value and possibly displacing the location of the maximum. That the contribution of the middle term to the delocalization index is negative can be verified by using the orthogonality of the 1s and the 2s orbitals. This represents a characteristic interference term found in wavelike behavior. Its contribution serves to decrease the values of the delocalization index.

To be more specific, choose the spatial parts of the orthonormal 1s and 2s orbitals to be

$$\varphi_{1s}(\boldsymbol{r}) = \left(\frac{Z_{1s}{}^3}{\pi}\right)^{1/2} e^{-Z_{1s}r}$$

and

$$\varphi_{2s}(\boldsymbol{r}) = \left[\frac{3Z_{2s}{}^5}{8\pi(4Z_{1s}{}^2 - 2Z_{1s}Z_{2s} + Z_{2s}{}^2)}\right]^{1/2}\left[\frac{1}{3}(Z_{1s} + Z_{2s}/2)r - 1\right]e^{-Z_{2s}r/2}$$

with the effective nuclear charges $Z_{1s} = 3.7$ and $Z_{2s} = 2.25$,

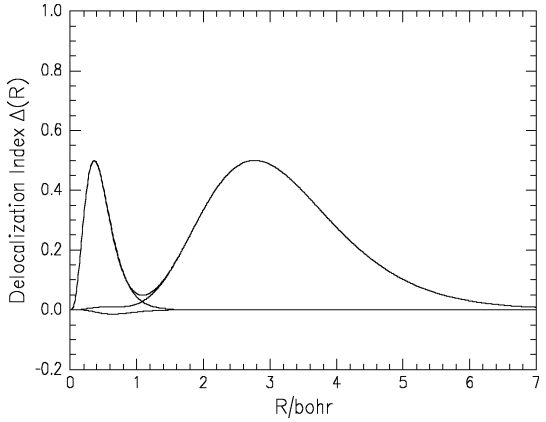

Figure 2. Simulated delocalization index of beryllium along with the 1s, 2s, and interference contributions.

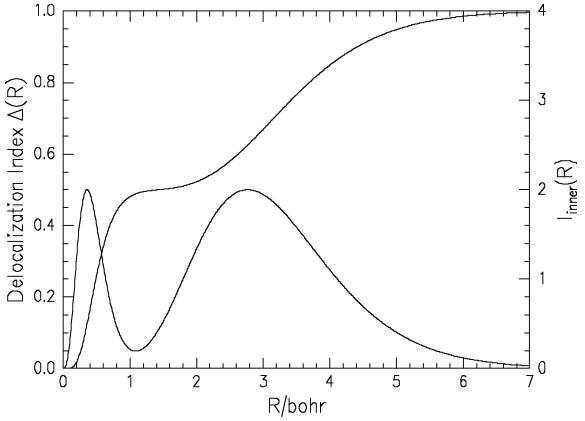

Figure 3. Simulated delocalization and self-sharing indices of beryllium.

the latter chosen so as to give approximate agreement with the delocalization index for beryllium given later in Figure 5.

The delocalization index $\Delta(R)$ along with the separate contributions from the 1s and the 2s orbitals and from the interference term are plotted in Figure 2 as a function of the radius R. The delocalization index is the top curve with two maxima. The contribution of the 1s orbital to $\Delta(R)$ is the curve with the single peak on the left. This contribution forms the main part of the first peak. The contribution of the 2s orbital to $\Delta(R)$ is the curve with the single peak to the right, the 2s orbital being essentially the sole contribution to the delocalization index for $R > 1.3$. The curve that is negative represents the contribution of the interference term. In the present example this term is small. However, we do note that in the region in which the 1s orbital is the major contributor, the 2s orbital makes but a small contribution, which is mainly canceled by the interference term.

The value of $\Delta(R)$ at each maximum is 0.50, the number of electrons in the shell which are actively shared across the surface of the sphere times the maximal value of the delocalization index for a single electron. This is amplified below when the self-sharing index is analyzed. The radius of the minimum simply gives the radius of the sphere across which the sharing is least—the electrons are essentially confined to the inner or to the outer region.

Although we have phrased the above in terms of the 1s, 2s, and interference contributions, these are not unique because, as is well-known, the orbitals themselves in the case of a single determinant wave function are not unique but may be transformed into other sets of orbitals by unitary transformations. It is the delocalization index which is unique.

Complementing the delocalization index, $\Delta(R)$ is the self-sharing index

$$I_{\text{inner}}(R) = \int_{|\mathbf{r}|,|\mathbf{r}'|\le R} d\zeta\, d\zeta'\, I(\zeta;\zeta')$$

which gives the number of electrons shared only to points within the inner region, hence localized within the inner region and not shared across the spherical boundary. This index, also invariant to unitary transformations of the orbitals, and the delocalization index obey the sum rule that the sum of the two gives the average number of electrons $N_{\text{inner}}(R)$ in the inner region

$$N_{\text{inner}}(R) = I_{\text{inner}}(R) + \Delta(R)$$

A plot of $I_{\text{inner}}(R)$ as a function of the radius of the sphere using the vertical scale on the right is given in Figure 3. The delocalization index is superimposed on the figure using the left scale. There are two regions of interest in the figure. The first is the region $0 \le R < 0.2$ in which the self-sharing index is essentially zero—all the electrons are shared to the outer region for these values of the radius—and the second is for $1.0 < R < 1.5$ in which the self-sharing index is essentially flat at a value of 2—the number of electrons in the 1s orbital. We note that this flat region occurs near and to the right of the minimum of the delocalization index. Any additional electrons in the inner region as R is increased from roughly a value of 1.1 are shared to the outer region; the electrons in the inner 1s region have lost their potency for further delocalization. The behavior in this second region serves to reinforce the idea that the electrons in the inner region are now spectators of the valence region and that the maximal values of the delocalization index in a region is the number of active electrons in that region (or shell) times the maximal value for a single electron, 0.25. Note also that this behavior also delineates the valence region in this example as beginning at roughly the radius of $R = 1.1$.

The other atoms in the first row of eight have contributions from p orbitals. Consider the case in which the natural spin−orbitals can be written as either pure s or pure p orbitals. Because the regions of integration are spherical, cross terms such as $(\varphi_{\text{ns}}, \varphi_{2p_x})_{|\mathbf{r}|\le R}$ and $(\varphi_{2p_x}, \varphi_{2p_y})_{|\mathbf{r}|\le R}$ vanish, so there is no interference between orbitals of different angular momenta. If the maxima of the contributions of the 2p orbitals are located at the same radius as the maximum of the 2s orbital, the value of the maximum is simply the number of electrons active in the shell times 0.25. For example, the outer (second) maximum of the delocalization index for neon is expected to be close to 2. But the maxima of the 2s and 2p orbitals need not be at the same location, resulting in a possible diminution of height of the maximum.

One additional reason exists for the maxima not being simply the number of active electrons in a shell times 0.25—a correlation that has been left out of the simplistic models just considered. When the delocalization index is written in terms of the natural spin−orbitals, eq 1, it is to be noted both that there are cross terms ($m \neq n$) that lead to negative contributions to the delocalization index and that there are fractional occupation numbers for the orbitals contributing to $\Delta(R)$, each of these influencing the heights of the maxima.

In the special case that the total orbital angular momentum L of the wave function is zero, the single particle density matrix $P_{LM}(\zeta;\zeta')$, normalized to the total number of electrons N, can

be written in terms of the spherical harmonics $Y_{lm}(\theta,\varphi)$ as (see the appendix)

$$P_{00}(\zeta;\zeta') = \sum_{l,m} Y_{lm}(\theta,\varphi)\, P_{00;l}(r,\sigma;r',\sigma') Y^*_{lm}(\theta',\varphi') \qquad (6)$$

which is diagonal in l and m. There is a similar decomposition of the sharing amplitude[9]

$$\langle\zeta;\zeta'\rangle = \sum_{l,\,m} Y_{lm}(\theta,\varphi)\, A_{00;l}(r,\sigma;r',\sigma') Y^*_{lm}(\theta',\varphi') \qquad (7)$$

with $A_{00;l}(r,\sigma;r',\sigma')$ the matrix square root of $P_{00;l}(r,\sigma;r',\sigma')$

$$P_{00;l}(r,\sigma;r',\sigma') = \sum_{\sigma''} \int \mathrm{d}r''\, r''^2 |A_{00;l}(r,\sigma;r'',\sigma'')\, A_{00;l}(r'',\sigma'';r',\sigma')$$

The result is that the delocalization index can be written as a sum of contributions of the different l values

$$\Delta(R) = \sum_l \Delta_l(R) \qquad (8)$$

with

$$\Delta_l(R) \equiv (2l+1) \sum_{\sigma,\sigma'} \int_{r\le R} \mathrm{d}r\, r^2 \int_{r'>R} \mathrm{d}r'\, r'^2 |A_{00;l}(r,\sigma;r',\sigma')|^2 \qquad (9)$$

Similarly, if the wave function is an eigenfunction of the z-component of the total spin, the z-component of the single particle spin commutes with the single particle density matrix with the result that the density matrix is diagonal in the spin variable

$$P(\zeta;\zeta') = P_\sigma(\boldsymbol{r};\boldsymbol{r}')\delta_{\sigma,\sigma'}$$

The α and β components of spin do not interfere and the contributions of up and down spin can be considered separately. The sharing amplitude can be similarly decomposed, and the contributions of the different spins to the delocalization index are additive.

III. Numerical Results for Atoms

In this section we give the results of numerical calculations for a number of atoms. The calculations were done using the GAUSSIAN 98 suite of programs[10] with, unless otherwise noted, the 6-31++G** basis at the QCISD level of approximation. The core electrons were included when correcting the Hartree−Fock results for electron correlation. Six d orbitals were included in all calculations and 10 f orbitals in those involving f orbitals. All calculations used the minimal nonrelativistic Hamiltonian.

The atomic overlap integrals used in the formation of the delocalization indices were calculated using a slightly modified version of PROAIMV[11] and then constructing $\Delta(R)$ according to eq 1. The modification was simply to ensure that the radius of the β sphere never exceeded the radius R. The points on the lines in all subsequent figures indicate the values of the radii at which the indices were calculated. The lines give the results of a cubic spline fit to the points.

The atoms considered in this section are lithium, beryllium, aluminum, the rare gases neon, argon, krypton, xenon, and radon, and the atoms zinc and gold. All atoms are in their ground state. The contributions of the up and down spin are given for lithium and for aluminum whereas the decomposition in terms of the various angular momentum components are given for beryllium, neon, argon, zinc, and gold. The self-sharing index for the inner sphere is given in the case of beryllium The delocalization indices for carbon, oxygen, nitrogen and silicon are given in conjunction with their hydrides in the next section. The delocalization index for phosphorus is given elsewhere.[9]

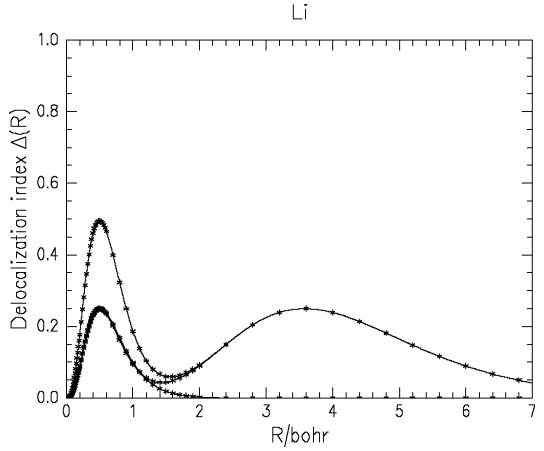

Figure 4. Delocalization index for lithium along with spin up and down contributions to $\Delta(R)$.

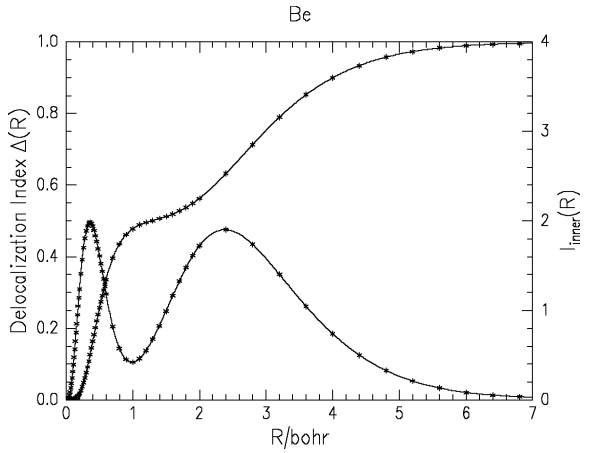

Figure 5. Delocalization and self-sharing indices for beryllium.

Li. The delocalization indices for lithium are given in Figure 4. The uppermost line is the total delocalization index, the next lower curve, which coincides with the upper curve at large radii, is the contribution of the α spins to the delocalization index whereas the remaining curve is the contribution of the β spin. To be noted is the coincidence of the α and β contributions at radii less than 1.2 bohr. These radii clearly lie in the core region. The β spin contribution is the lesser contribution at radii greater than 1.5 bohr and, for all practical purposes, vanishes by a radius of 2 bohr. The valence region is quite clearly that region extending from 1.5 bohr outward. The value of the delocalization index at the inner maximum is 0.5 whereas that of the outer maximum is 0.25, both values as anticipated by the argument given in the previous section.

Be. The delocalization index (scale on the left) and the self-sharing index for the inner sphere (scale on the right) for beryllium are given in Figure 5. The curves are remarkably similar to those of Figure 3. (The effective nuclear charges used for Figure 3 were adjusted to make the maxima of the delocalization index occur at roughly the same radii.) The value of the maximum of the inner peak of the delocalization index is 0.5, the naive value for two active electrons, whereas the outer peak has a maximum of 0.476 at a radius of 2.38 bohr,

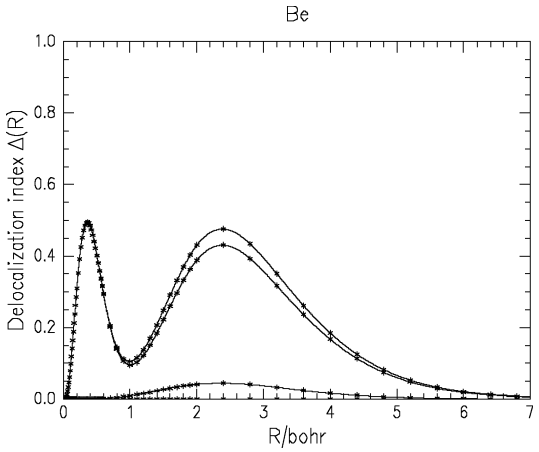

Figure 6. Angular momentum contributions to $\Delta(R)$ for beryllium.

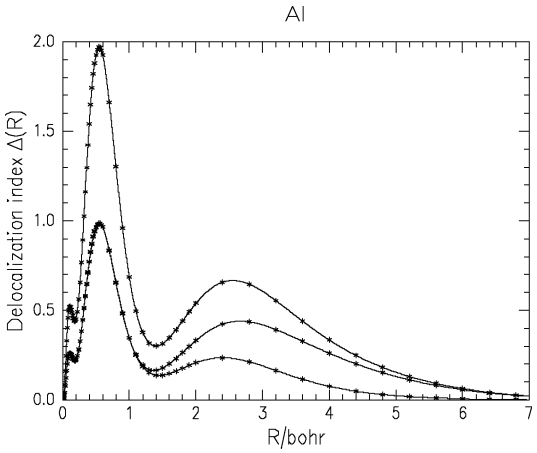

Figure 7. Delocalization index for aluminum together with the spin up and down contributions to $\Delta(R)$.

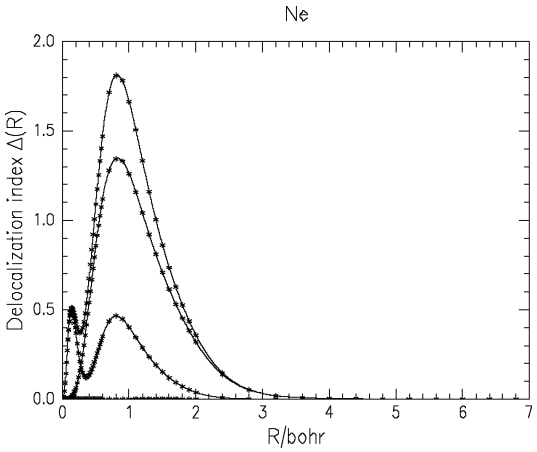

Figure 8. Delocalization index of neon with angular momentum contributions.

somewhat less than the value of 0.5 anticipated on a naive basis. Compared to the maxima found for the delocalization index in the lithium atom, the maxima for beryllium have moved to smaller radii, a result of the greater nuclear charge of Be. The self-sharing index has the characteristics noted in the previous section. There is a short horizontal section from the origin to a radius of about 0.2 bohr, followed by a steep increase until the radius is roughly 1.0 bohr followed by a relatively flat region extending to 1.5 bohr. This latter region of lesser slope indicates that the additional electrons added to the inner sphere as the radius is increased are active electrons in the sense of being shared to the outer region, as reflected in the growth of $\Delta(R)$ in this region. As the radius is extended into the region of the second shell, the self-sharing index increases until it reaches the maximum number of electrons in the atom.

One effect of correlation on the delocalization index can be quite simply checked in this atom. At the Hartree−Fock level of approximation the atomic orbitals are pure $l = 0$ orbitals, and these are the only contributors to the delocalization index. When correlation is taken into account, orbitals of other angular momenta can contribute to the delocalization index. Because the ground state has a total orbital angular momentum of zero, the delocalization index can be written as a sum of noninterfering contributions of single particle orbital angular momenta, eq 8. The top curve in Figure 6 is the total delocalization for beryllium as given before. The next two lower curves give the $l = 0$ and $l = 1$ contributions to $\Delta(R)$. (The $l = 2$ contribution, essentially coinciding with the abscissa, is negligible at this level of approximation.) The largest contribution to $\Delta(R)$ is from $l = 0$ orbitals. As may be expected on the basis of a lack of a 1p orbital in hydrogen-like molecules, the $l = 1$ orbitals make essentially no contribution in the region of the maximum closest to the nucleus. But, in the region of the outer maximum the $l = 1$ contributions are not insignificant, the contribution of the $l = 1$ contribution being about 10% that of the $l = 0$ contribution at a radius of 2.4 bohr.

Al. Figure 7 gives the delocalization index for aluminum as well as the α and β spin contributions. Consider first the total delocalization index, the highest of the three curves. The contribution of the 1s shell is apparent, giving the leftmost peak. It is to be noted that the peak height is 0.524, about 5% larger than naively expected. This peak, however, is riding on the beginnings of the next shell. The maximum of the second peak is 1.970, somewhat less than the naive expectation of 2 for eight electrons in a shell. The maximum of the third peak, occurring at a radius of 2.55 bohr, is 0.667, significantly less that the simple value of 0.75.

The contributions of the α and β spins to the total delocalization index are the lower two curves in the figure. The two curves are indistinguishable at radii less than 1.2, these radii being in the core region. The divergence occurs in the valence region.

A part of the reason for the discrepancy of the maximum value of the delocalization index from the value of 0.75 in the outer region is that the contributions of the α and β spins occur at different radii, the maximum value of the α spin contribution is 0.440 at a radius of 2.67 bohr, whereas the values of the β spin contribution give a maximum of 0.236 at a radius of 2.40 bohr. The maxima do not coincide, reducing the value from 0.75 and, in addition, the values of maxima of the α and β contributions are less than the naively anticipated values of 0.50 and 0.25.

There is further information that can be gleaned from the figures. In the outer region the β spin contribution is expected to be mainly due to a 3s orbital, whereas the α spin contribution is due to both a 3s orbital and a 3p orbital. If the α and β 3s orbitals are similar in shape, we infer that, in terms of the delocalization index, the 3p orbital extends to a larger radius, in terms of sharing, than the 3s orbital.

The next set of atoms considered constitutes the rare gases. In addition to the total delocalization index, the plots for neon and argon also contain the contributions of the angular momenta $l = 0$, 1, 2 to $\Delta(R)$.

Ne. Figure 8 gives the delocalization indices for neon. The upper curve is the total delocalization index. The next lower

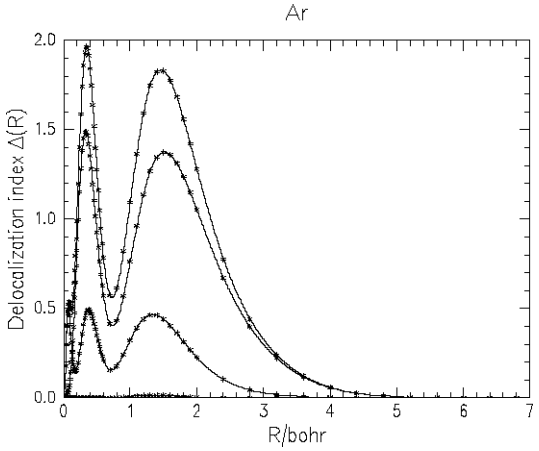

Figure 9. Delocalization index of argon with angular momentum contributions.

curves are the contributions of angular momentum $l = 1$ and $l = 0$, in descending order, to the delocalization index. The lowest curve (essentially the baseline) is the contribution of the orbitals with $l = 2$. The first peak in the total delocalization index has a maximum value slightly greater that 0.5, this being the 1s orbital contribution on top of minor contributions from the 2s and 2p orbitals. The second maximum has a value of 1.813 at a radius of 0.82. This is about 10% lower than the naive expectation of 2 for eight electrons in the shell. The curves giving the p and the s contributions in this region are each lower than the anticipated values of 0.5 and 1.5, the most significant discrepancy being in the $l = 1$ curve. The maximum of the p contribution lies to the right of that of the s contribution and the tail of the p contribution extends considerably to the right of the *s* contribution. As found below, this is a consistent theme in the rare gas atoms.

Ar. The trends established for neon continue in argon, the delocalization index and the angular momentum contributions being given in Figure 9. In the core region, the values of the maxima are close to the anticipated values of 0.5 and 2.0, for the contributions of 2 and, respectively, 8 electrons. The inner maximum, although still a maximum, is merging into the rise to the second maximum. As found below, this merging of a maximum with the next outer maximum continues in the heavier rare gas atoms. The maximum value of the delocalization index of the outer shell is, as in neon, smaller than the value of 2, being 1.835 at a radius of 1.46 bohr. In this case some of the discrepancy is due to the noncoincidence of the maxima of the s and the p contributions to the index, the maxima of these two contributions being at radii of 1.34 and 1.51 bohr, respectively. In addition, there are the undoubted effects of correlation on the sharing of electrons in this outer shell because the maxima of the s shell and the p shell contributions are 0.466 and 1.375, the latter being some 10% lower than the expectation based on simple counting of electrons in a subshell. The d orbitals make a very small, barely visible contribution to $\Delta(R)$ in this atom, with the maximum value of the contribution occurring in the region of 1.4 bohr.

Kr, Xe, and Rn. Figures 10−12 give the delocalization indices for krypton, xenon, and radon. In addition, the contributions of the different single particle orbital angular momenta to $\Delta(R)$ are given for radon, this being the first atom of the paper which has f electrons. The basis set for xenon is taken from Huzinaga et al.[12,13] augmented by a diffuse d orbital. The basis set used in the radon calculation is taken from Gropen[12,14] supplemented by an added diffuse d orbital from Huzinaga et al.[15]

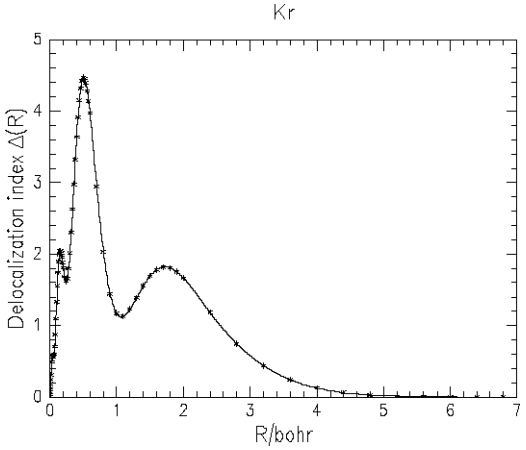

Figure 10. Delocalization index of krypton.

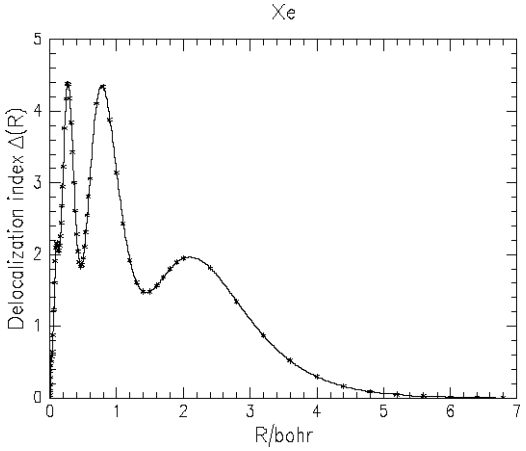

Figure 11. Delocalization index of xenon.

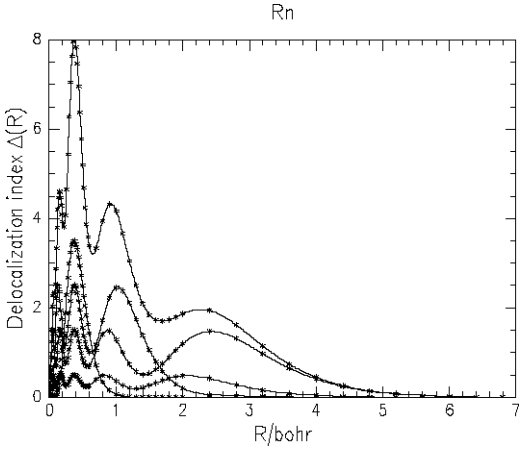

Figure 12. Delocalization index of radon with angular momentum contributions.

In each of the three atoms the maximum formerly associated with the innermost shell now appears as a distinct shoulder on the rise to the maximum associated with the second shell. This completes the trend noted in connection with argon. In addition the second shell in radon is also associated with a shoulder rather than a maximum, extending the trend to more shells as heavier atoms are considered. Nonetheless, as illustrated in Figure 13, which gives the delocalization index in the vicinity of the origin on an expanded scale, the locations of the inner regions are clearly discernible, making the number of shells countable.

In agreement with the number of shells assigned classically, for krypton there are a total of four distinct shoulders or maxima,

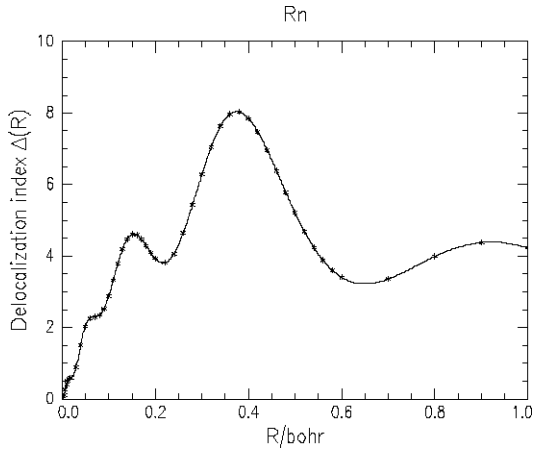

Figure 13. Delocalization index of radon near the origin.

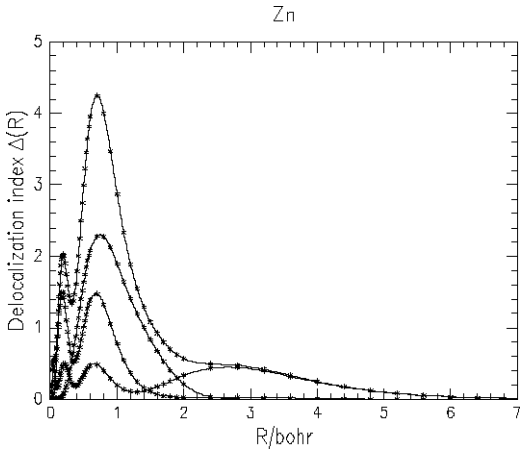

Figure 14. Delocalization index of zinc with angular momentum contributions.

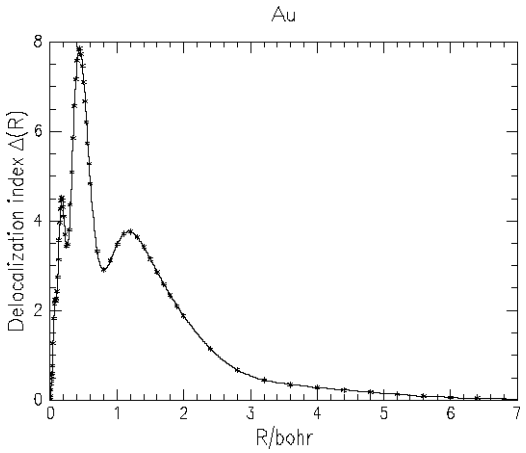

Figure 15. Delocalization index of gold.

five in the case of xenon and six in the case of radon. The heights of the maxima and of the shoulders of the delocalization indices follow approximately the simple rule of being the number of electrons in a shell times 0.25. The contribution of the $l = 3$ electrons to the delocalization index in radon in addition to those of smaller l is apparent in the maximum having a height of 8, which occurs at about 0.4 bohr. In addition to the merging of the inner shells in this series to form shoulders in place of distinct maxima, the increasing nuclear charge results in the drift of the shells to smaller radii.

The contributions of the various angular momenta to the delocalization index in radon are also given by the lower curves in Figure 12. Of note are the locations of the maxima of the contributions of the different angular momenta. In the outermost shell region, the maximum of the p contribution occurs at a radius of about 2.4 bohr whereas that of the s contribution occurs at about 2.0 bohr, a significant difference between the two. In the next region inward, the maxima of the $l = 0$, 1, and 2 contributions are similarly ordered with the maximum of the d contribution being at the largest radius.

There is one cautionary note to be mentioned here when interpreting the contribution of the f functions to the delocalization index. There is only one contracted set of f functions in the basis set for radon. Therefore the shape of this contribution to the delocalization index is the same as that found at the Hartree−Fock level of approximation.

The last two atoms considered are zinc and gold. Spin−orbit coupling has been ignored in the calculation of the one-particle density matrix, and hence in the delocalization index. As a result, the total orbital angular momentum of the wave function vanishes, $L = 0$, and we can separate the contributions of the various single particle angular momenta to the delocalization indices, just as in the case of the rare gas atoms.

Zn. The delocalization index for zinc, as well as the $l = 0$, 1, and 2 contributions to $\Delta(R)$, are given in Figure 14. The basis set is taken from Rasolov et al.[12,16] The comments made previously about the values of the maxima apply here. Use of an expanded abscissa shows that there is a valley, small but distinct, at a radius of 0.05 bohr, this valley separating the 1s shell from the 2s2p shell. The $n = 2$ and $n = 3$ shells are separated by a distinct valley, with the values of the maxima indicating that 8 and 18 reside in the shells. Beyond a radius of about 2.2 bohr there is a plateau of height very close to 0.5 extending to a radius of about 3.0 bohr. This is followed by a decline as the radius is increased.

The contributions to the delocalization index from the various angular momenta give the three inner core $l = 0$ shells as lying between the origin and a radius of about 1.25 bohr, The two $l = 1$ shells lie between the origin and roughly a radius of 1.6 bohr. The $l = 2$ shell, which has a distinct horizontal region near the origin (related to the r^2 dependence of the $l = 2$ orbitals in the neighborhood of the origin), extends to about 2.4 bohr, with a good deal of delocalization lying beyond the $l = 1$ contributions. In the outer region, beyond a radius of 1.25 and extending to a considerable distance, lies the final $l = 0$ shell with a maximum of about 0.5. This final s shell is well outside the other contributions to the delocalization index and is the major contributor to the plateau mentioned above. We note that the maxima of the third s, the second p, and the d contributions form a progression, in that order, to larger radii.

Au. The delocalization index for gold, using the nonrelativistic basis set of Jansen,[17] is given in Figure 15. The delocalization index associated with the inner two shells appear as shoulders on the first maximum, which occurs at a radius of about 0.2 bohr (see Figure 17 below for an expanded view). The height of this maximum is close to 4.5, the value expected by the simple counting game for a shell containing 18 electrons. The next maximum has a height of 8.02, again corresponding to the value from the counting game for a shell containing 32 electrons. The maximum at the radius of about 1.2 bohr is followed by a long slow decline beginning at a radius of about 3.2 bohr.

That the major (but not only) contribution to the delocalization index in the region beyond 3.2 bohr is from angular momentum $l = 0$ is apparent from Figure 16, which gives the contributions of the various angular momenta to $\Delta(R)$. However, it should

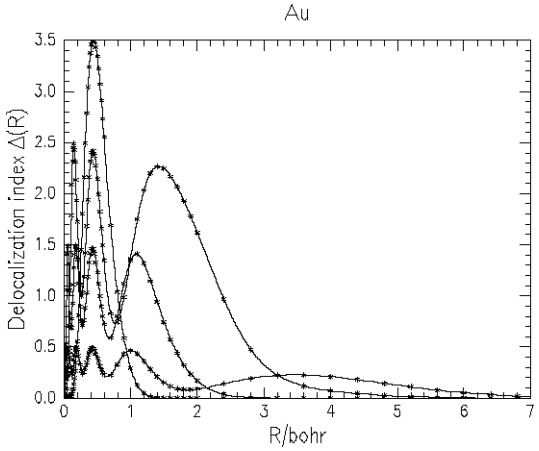

Figure 16. Angular momentum contributions to the delocalization index of gold.

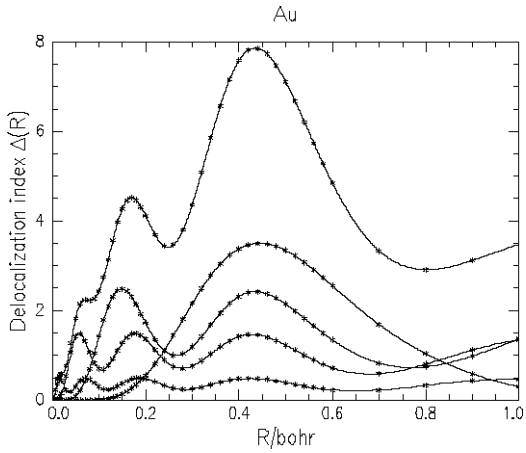

Figure 17. Delocalization index of gold near the origin with angular momentum contributions.

be noted that the tail of the rightmost $l = 2$ contribution to the delocalization index (conventionally the 5d contribution) extends well into the region of this s contribution. This is unlike the behavior in Zn in which the delocalization index in the outermost region stems entirely from an $l = 0$ contribution.

Of note in the decomposition by angular momenta are the rightmost maxima of the $l = 2$ and $l = 1$ contributions as well as the penultimate maximum of the $l = 0$ contributions. These maxima occur at increasing values of the radius in the order of increasing values of l. We note that the 4d shell has a considerable overlap with the 6s shell, although the 6s contribution is dominant at large radii. Also to be noted is the $l = 3$ contribution which resides within the fourth shell. These features can, of course, be found by other means, e.g., at the Hartree−Fock level of approximation by transforming the natural spin−orbitals to orbitals of definite angular momentum. The present results, however, have been found using a correlated wave function and it is nice to see the shell structure appear by using invariant sharing quantities with a correlated wave function.

The contributions of the various components of angular momentum to the delocalization index for small R are not clear in Figure 16. The total delocalization index as well as the angular momentum contributions are given using an expanded scale near the origin in Figure 17. We note that maximum of the 2p contribution occurs at a smaller radius than that of the 2s contribution. Similarly, the maximum of the 3d contribution is at a smaller radius than that of the 3p contribution which in turn is at a smaller radius than the 3s contribution. When maxima of the angular momentum contributions to the fourth shell are compared, it is found that the order of the radii is reversed, the ordering now being, from smallest radius to largest, 4s, 4p, 4d, and then 4f.

TABLE 1: Radius of the Beginning of the Valence Region for Selected Atoms

atom	R_{valence}
Li	1.6
Be	1.0
C	0.6
N	0.5
O	0.4
Al	1.4
P[9]	1.0
Zn	1.9
Au(6s)	3.2

The cautionary note given in the case of radon also applies to gold—namely, that there is only one contracted set of f functions in the basis set for gold. Therefore the shape of this contribution to the delocalization index is the same as that found at the Hartree−Fock level of approximation.

The approximate radii which mark the beginning of the valence regions for some of the atoms are given in Table 1. The radii for carbon, nitrogen, and oxygen are taken from the figures in next section whereas that for phosphorus is taken from ref 9. It is apparent from the figures that the radii for Li through Zn are reasonably well delineated whereas the radius for Au is not. The radius given for Au is the radius at which the s contribution becomes larger than the d contribution to the delocalization index. Note the contrast between zinc and gold. In Zn the beginning of the region for the outermost $l = 0$ contributions is fairly clear, roughly at 1.9 bohr. The situation in Au, as just noted, is more murky for there is considerable overlap of the tail of the outermost $l = 2$ region with the large distance contribution of the $l = 0$ region. Is this possibly related to the variety of oxidation states that exist for gold?

IV. Numerical Results for Molecules

At the outset one motivation for the determination of the delocalization structure of atoms in molecules was to compare the sum of the carbon−hydrogen sharing indices to the carbon atom in methane delocalization indices evaluated at radii in the range of the distance of the bond points from the carbon nucleus, this possibly providing a check on the sensitivity of the sharing indices to the location of the boundaries of the basins. Another motivation for determining the delocalization structure of the electrons in atoms is to determine the valence region of atoms so that the fixed points used in conjunction with the sharing amplitudes can be properly positioned to give the behavior of the electrons in the bonding regions of a molecule. In addition, the influence attached atoms have on the delocalization from the core region of an atom should be ascertained. In this section we consider the delocalization index of the four hydrides CH_4 (together with CH_4 at the Hartree−Fock level of approximation), NH_3, H_2O, and SiH_4.

CH_4. The delocalization index about the central atom in CH_4 is given in Figure 18, along with the delocalization in an isolated carbon atom (the lower of the two curves). First we note that in the core region, radii less than 0.5 bohr, the delocalization index of the carbon atom and that of the carbon atom in methane are indistinguishable. It is for larger radii that the indices differ, and it is this which is a verification of the location of the valence region of a carbon atom.

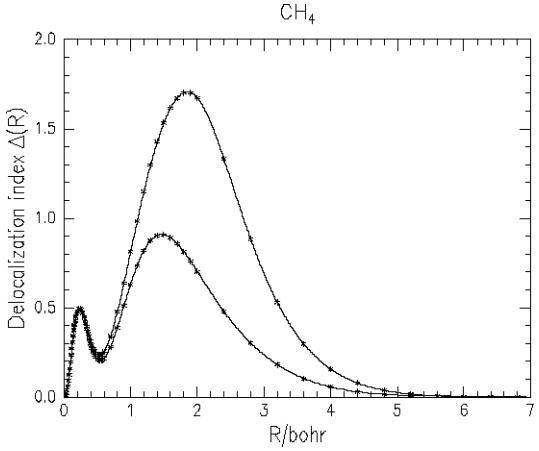

Figure 18. Delocalization indices for carbon in methane (higher curve) and of a carbon atom.

TABLE 2: Sharing Indices for CH_4

basin	C	H1	H2	H3	H4
C	4.172				
H1	0.424	0.553			
H2	0.424	0.018	0.553		
H3	0.424	0.018	0.018	0.553	
H4	0.424	0.018	0.018	0.018	0.553

The basin sharing indices for methane are given in Table 2. The diagonal entries give the self-sharing indices of the atoms (the numbers following the atom symbols identify the atomic basins by number) whereas the off-diagonal entries give the interbasin sharing indices. Only the diagonal entries and those below the diagonal are given. The entries above the diagonal simply reproduce the indices already given. It is clear from the table that the primary interbasin sharing is between the carbon basin and the hydrogen basins.

The bond points as defined by Bader[2] lie at about 1.38 bohr from the carbon nucleus. The delocalization index $\Delta(R)$ for a radius of 1.38 bohr is about 1.40 whereas the sum of the four C−H sharing indices is about 1.72, considerably greater than the delocalization index for the central atom. In fact, the maximum of $\Delta(R)$ is 1.70 and this occurs not near the bond points but near a radius which corresponds to the distance between the carbon nucleus and a proton. The reason for the difference is that the carbon basin is far from spherical[18] and that there is more surface area between the carbon basin and the hydrogen basins than given by a spherical surface.

The maximum value of the delocalization index for the carbon atom is 0.90, about 10% less than the simple counting argument gives. Now the index in methane contains the four electrons supplied by the hydrogens. The naive calculation gives a value of the maximum as 2, whereas Figure 18 gives a maximum of 1.7, 15% less than the naive calculation gives. Is this due to the nonspherical nature of methane or to correlation? Figure 19 gives the delocalization index for methane at the Hartree−Fock level of approximation (upper curve) and at the QCISD level of approximation using the same basis set as above. The core region is remarkably similar to that from the QCISD level of approximation despite the core electrons being included when determining the correlated amplitude. The outer region differs in the Hartree−Fock calculation, with the maximum in the valence region being 1.97, essentially the value from the naive counting. Clearly the main reason for the decrease in the maximum value in the QCISD calculation from the naive value is the inclusion of correlation.

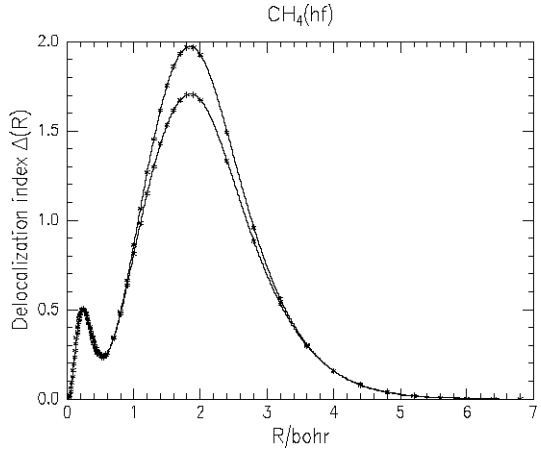

Figure 19. Delocalization indices for carbon in methane. Higher curve is from a Hartree−Fock calculation.

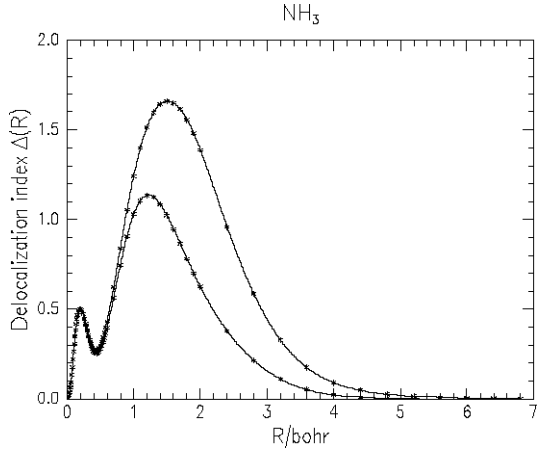

Figure 20. Delocalization indices for nitrogen in ammonia and of a nitrogen atom.

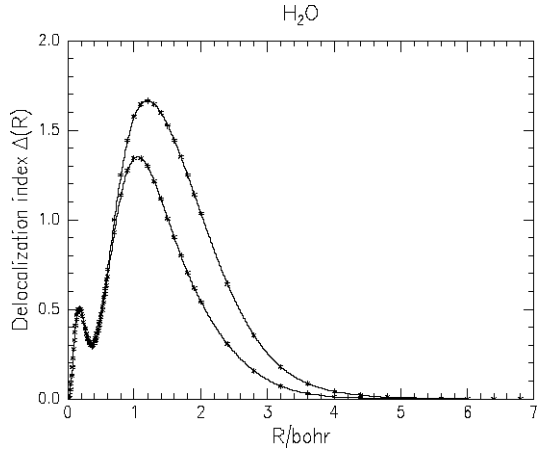

Figure 21. Delocalization indices for oxygen in water and of an oxygen atom.

NH_3 and H_2O. The delocalization indices of nitrogen and oxygen (lower curves in Figures20 and 21) illustrate both the effects of increased nuclear charge and the increased number of valence electrons when compared to the delocalization index for carbon. The increased nuclear charge in the sequence C to N to O draws the maxima of the delocalization index increasingly toward the nucleus. The increase in the number of valence electrons results in systematic increase in the height of the maxima of the delocalization indices in the valence regions.

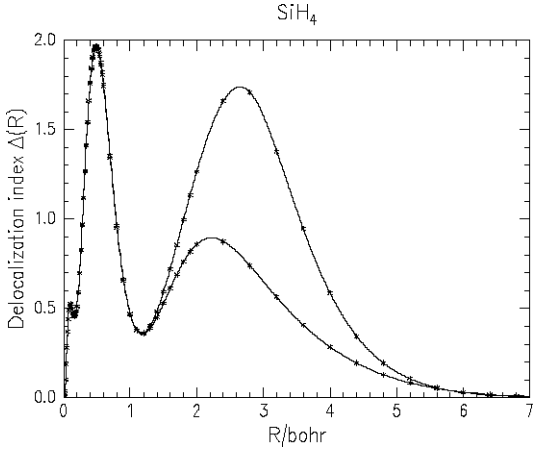

Figure 22. Delocalization indices for silicon in silane and of a silicon atom.

There are some differences and some similarities between the three hydrides considered so far. In methane, Figure 18, the delocalization index of the molecule begins to diverge from that of the carbon atom at the minimum that occurs at 0.6 bohr. In ammonia, Figure 20, the divergence between the delocalization indices becomes noticeable about one-third the way up the slope in the valence region. In water, Figure 21, the divergence occurs somewhat beyond the halfway up the slope in the valence region. Similarly, the heights of the maxima of the delocalization indices of the three atoms increases in the order of the increasing number of electrons in the valence region.

The delocalization indices are similar in that the heights of the maxima of the delocalization indices of all three maxima are essentially the same, the maxima in the valence regions being close to 1.7, apparently reflecting the fact that the total number of bonding and lone pair electrons in the valence region is the same in all three molecules.

SiH_4. The last molecule we consider is SiH_4. The delocalization index for Si and for Si in the molecule is given in Figure 22. In the core region the delocalization indices are virtually indistinguishable. There are two maxima in the core region, corresponding to principal quantum numbers of 1 and 2, with the values of the maxima being in agreement with the naive counting. As could be anticipated from the atoms and molecules in the preceding row, it is in the valence region that the indices for the silicon atom and the silicon atom in the molecule diverge. The core region, now containing two shells, remains intact as the molecule is formed. As in methane, the maximum value of the rightmost peak in the molecule is less than the canonical 2, being close to the 1.7 found in the other three hydrides. It is to be noted that the two delocalization indices plotted in Figure 22 begin to diverge at the beginning of the valence region, similar to what is found in methane, the other tetrahydride considered.

V. Conclusions

The point to point sharing amplitudes $\langle\zeta;\zeta'\rangle$ and indices $I(\zeta;\zeta')$ introduced in ref 1 give quantitative measures of the sharing (delocalization) of a single electron between the two points ζ and ζ' in a single or a many electron system. ($I(\zeta;\zeta')$ is normalized to the total number of electrons in the system being considered.) In this paper we investigate the delocalization of an electron in single atoms and about the central atom of some simple molecules by means of an atom delocalization index $\Delta(R)$. This index is given by a double integral of the sharing index $I(\zeta;\zeta')$ over the two indices ζ and ζ'; ζ over an inner spherical region of radius R centered on a nucleus and ζ' over the region exterior to that spherical region. The result is that we have a measure of the delocalization of the electrons between the inner and outer regions of an atom. We also make modest use of an associated self-sharing index, an index that is a measure of the number of electrons shared to points within the inner spherical region.

As a function of the radius R, $\Delta(R)$ shows remarkable shell-like behavior in atoms, with, for the lighter atoms, delineations between the shells marked by distinct minima in $\Delta(R)$. For the heaviest atoms considered, the separation between inner shells is marked not by minima but rather by distinct plateaus. The values of the maxima in the atom delocalization index, which when multiplied by 4 give the number of electrons shared across the dividing spherical surface, are in close agreement with the "classical" number of electrons in the corresponding shell. The origin of this relation and reasons for deviations from the strict application of this relation is found in the influence of interference effects and in the correlation of the electrons relative to the Hartree−Fock approximation.

If the total orbital angular momentum of the atom is zero, the contributions to $\Delta(R)$ can be broken into a sum of contributions from the various single electron angular momenta with no interference terms. Similarly, if the total wave function is an eigenfunction of the z-component of the spin angular momentum, the contributions of the "up" and "down" spins can be separately considered. Just as the delocalization index shows the shell structure of an atom, so do the angular momentum and spin contributions to the delocalization index. However, we now find that the positions of maxima of the contributions of the different angular momenta need not coincide, this contributing to the discrepancy between a naive counting of the electrons and the values of the maxima of $\Delta(R)$.

Important for the application of the sharing amplitude to the determination of the behavior of electrons in bonding regions of molecules is the identification of the valence region of an atom. It is shown that the shell structure of $\Delta(R)$ gives the valence regions of atoms, thus allowing for the placement of the fixed points when using sharing amplitudes when investigating the behavior of electrons in molecules.

The delocalization indices about the heavy atom in several simple hydrides are given. These illustrate the invariance of the core electron structure of an atom upon bond formation, the changes in the valence region upon bond formation, and, for methane, the marked influence of electron correlation on the carbon atom delocalization in the outer regions of the molecule.

Acknowledgment. Parts of this paper are based on the Ph.D. dissertation of Petar M. Mitrasinovic, which was submitted to the Department of Chemistry and Biochemistry of Florida State University. All the calculations have been redone by the author.

Appendix

In this appendix we demonstrate that, when the total orbital angular momentum is zero, the single density matrix (normalized to 1) can be decomposed as

$$\rho_{00}(\zeta;\zeta') = \sum_{l,m} Y_{lm}(\theta,\varphi)\, \rho_{00;l}(r,\sigma;r',\sigma')\, Y^*_{\mathrm{lm}}(\theta',\varphi') \tag{A1}$$

i.e., is diagonal in the indices l and m.

Let the N-particle state $\Psi_{LM}(\zeta)$ be an eigenfunction of the z-component of angular momentum $\hat{L}_z$ and the square of the angular momentum $\hat{L}^2$,

$$\hat{L}_z\Psi_{LM}(\zeta^N) = \Psi_{LM}(\zeta^N)M$$

$$\hat{L}^2\Psi_{LM}(\zeta^N) = \Psi_{LM}(\zeta^N)L(L+1) \quad \text{(A2)}$$

with $\hbar = 1$. The single particle density matrix (normalized to 1) is defined by

$$\rho_{\mathrm{LM}}(\zeta;\zeta') \equiv \int d\zeta^{N-1}\Psi_{\mathrm{LM}}(\zeta,\zeta^{N-1})\Psi^*_{LM}(\zeta',\zeta^{N-1}) \quad \text{(A3)}$$

We begin by noting that because $\Psi_{LM}(\zeta,\zeta^{N-1})$ is an eigenfunction of $\hat{L}_z$ with eigenfunction M,

$$\int \mathrm{d}\zeta^{N-1}\, \hat{L}\Psi_{LM}(\zeta,\zeta^{N-1})\, \Psi^*_{LM}(\zeta',\zeta^{N-1}) = \int \mathrm{d}\zeta^{N-1}\, \Psi_{LM}(\zeta,\zeta^{N-1})[\hat{L}_z\Psi^*_{LM}(\zeta',\zeta^{N-1})]^* \quad \text{(A4)}$$

The total angular momentum may be written as the sum of the angular momentum of particle 1, $\hat{l}$, and the contribution of the remaining particles to the angular momentum, $\Delta\hat{L}$

$$\hat{L} = \hat{l} + \Delta\hat{L} \quad \text{(A5)}$$

Because $\Delta\hat{L}$ is Hermitian

$$\int \mathrm{d}\zeta^{N-1}\, \Delta\hat{L}\Psi_{LM}(\zeta,\zeta^{N-1})\, \Psi^*_{LM}(\zeta',\zeta^{N-1}) = \int \mathrm{d}\zeta^{N-1}\, \Psi_{LM}(\zeta,\zeta^{N-1})[\Delta\hat{L}_z\Psi^*_{LM}(\zeta',\zeta^{N-1})]^* \quad \text{(A6)}$$

and we are left with

$$\hat{l}_z\hat{\rho} = \hat{\rho}\hat{l}_z \quad \text{(A7)}$$

The general expansion of the single particle density matrix in terms of the spherical harmonics $Y_{lm}(\theta,\varphi)$ is

$$\rho_{LM}(\zeta;\zeta') = \sum_{l,m,l'm'} Y_{lm}(\theta,\varphi)\, \rho_{LM;lm,l'm'}(r,\sigma;r',\sigma')\, Y^*_{l'm'}(\theta',\varphi') \quad \text{(A8)}$$

Because $\hat{l}_z$ and $\hat{\rho}$ commute, the terms with $m \neq m'$ vanish and the expansion reduces to

$$\rho_{LM}(\zeta;\zeta') = \sum_{l,m,l'} Y_{lm}(\theta,\varphi)\, \rho_{LM;lm,l'm}(r,\sigma;r',\sigma')Y^*_{l'm}(\theta',\varphi') \quad \text{(A9)}$$

We now consider the special case of zero total orbital angular momentum, $L = 0$. In this case the wave function is also an eigenfunction of the x- and y- components of the total orbital angular momentum,

$$\hat{L}_x\Psi_{LM}(\zeta^N) = \Psi_{LM}(\zeta^N) \times 0$$

$$\hat{L}_y\Psi_{LM}(\zeta^N) = \Psi_{LM}(\zeta^N) \times 0 \quad \text{(A10)}$$

and we find that the single particle density matrix commutes with both $\hat{l}_x$ and $\hat{l}_y$. As a consequence, the single particle density matrix commutes with the square of $\hat{l}^2$

$$\hat{l}^2\hat{\rho} = \hat{\rho}\hat{l}^2 \quad \text{(A11)}$$

This leads to

$$\sum_{l,m,l'} [l(l+1) - l'(l'+1)]Y_{lm}(\theta,\varphi)\, \rho_{00;lm,l'm}(r,\sigma;r',\sigma')Y^*_{l'm}(\theta',\varphi') = 0 \quad \text{(A12)}$$

whence, because the spherical harmonics are independent, $\rho_{00;lm,l'm}$ is diagonal in l and l'

$$\rho_{00;lm,l'm} = \rho_{00;lm}\delta_{ll'} \quad \text{(A13)}$$

Also from the fact that the x- and y-components of the orbital angular momentum commute with the density matrix it follows that $\hat{l}_+ \equiv \hat{l}_x + i\hat{l}_y$ commutes with the density matrix. This leads to the relation

$$\sum_{l,m}[(l-m)(l+m+1)]Y_{lm}(\theta,\varphi)\, Y^*_{l'm}(\theta',\varphi')[\rho_{00;lm}(r,\sigma;r',\sigma') - \rho_{00;l,m+1}(r,\sigma;r',\sigma')] = 0$$

which gives the recursion relation

$$\rho_{00;lm+1}(r,\sigma;r',\sigma') = \rho_{00;lm}(r,\sigma;r',\sigma')$$

indicating that $\rho_{00;lm}(r,\sigma;r',\sigma')$ is independent of m. The density matrix in this case is

$$\rho_{00}(\zeta;\zeta') = \sum_{l,\,m} Y_{lm}(\theta,\varphi)\, \rho_{00;l}(r,\sigma;r',\sigma')\, Y^*_{lm}(\theta',\varphi') \quad \text{(A14)}$$

References and Notes

(1) Fulton, R. L. *J. Phys. Chem.* **1993**, *97*, 7516.

(2) Bader, R. F. W.; Anderson, R. G.; Nguyen-Dang, T. T. *Isr. J. Chem.* **1980**, *19*, 8.

(3) Fulton, R. L.; Mixon, S. T. *J. Phys. Chem.* **1993**, *97*, 7530.

(4) Fulton, R. L.; Mixon, S. T. *J. Phys. Chem.* **1995**, *99*, 9768.

(5) Fulton, R. L.; Perhacs, P. *J. Phys. Chem.* **1998**, *102*, 8988.

(6) Fulton, R. L.; Perhacs, P. *J. Phys. Chem. A* **1998**, *102*, 9001.

(7) Löwdin, P. O. *Phys. Rev.* **1995**, *97*, 1474.

(8) Equation 3 of ref 1, with the volume *A* identified as the inner spherical region and the volume *B* identified as the remaining volume.

(9) Fulton, R. L. Comment on "Qualitative Characterization of the P−C Bonds in Ylides of Phosphorus". *J. Phys. Chem. A* **2004**, *108*, 11855.

(10) Frisch, M. J.; Trucks, G. W.; Schlegel, H. B.; Scuseria, G. E.; Robb, M. A.; Cheeseman, J. R.; Zakrzewski, V. G.; Montgomery, J. A., Jr.; Stratmann, R. E.; Burant, J. C.; Dapprich, S.; Millam, J. M.; Daniels, A. D.; Kudin, K. N.; Strain, M. C.; Farkas, O.; Tomasi, J.; Barone, V.; Cossi, M.; Cammi, R.; Mennucci, B.; Pomelli, C.; Adamo, C.; Clifford, S.; Ochterski, J.; Petersson, G. A.; Ayala, P. Y.; Cui, Q.; Morokuma, K.; Malick, D. K.; Rabuck, A. D.; Raghavachari, K.; Foresman, J. B.; Cioslowski, J.; Ortiz, J. V.; Baboul, A. G.; Stefanov, B. B.; Liu, G.; Liashenko, A.; Piskorz, P.; Komaromi, I.; Gomperts, R.; Martin, R. L.; Fox, D. J.; Keith, T.; Al-Laham, M. A.; Peng, C. Y.; Nanayakkara, A.; Challacombe, M.; Gill, P. M. W.; Johnson, B.; Chen, W.; Wong, M. W.; Andres, J. L.; Gonzalez, C.; Head-Gordon, M.; Replogle, E. S.; and Pople, J. A. *Gaussian 98*, Revision A.9; Gaussian, Inc.: Pittsburgh, PA, 1998.

(11) Biegler-Konig, F. W.; Bader, R. F. W.; Tang, *J. Comput. Chem.* **1982**, *13*, 317

(12) Basis sets were obtained from the Extensible Computational Chemistry Environment Basis Set Database, Version 6/19/03, as developed and distributed by the Molecular Science Computing Facility, Environmental and Molecular Sciences Laboratory, which is part of the Pacific Northwest Laboratory, P.O. Box 999, Richland, WA 99352, and funded by the U.S. Department of Energy. The Pacific Northwest Laboratory is a multiprogram laboratory operated by Battelle Memorial Institute for the U.S. Department of Energy under contract DE-AC06-76RLO 1830. Contact David Feller or Karen Schuchardt for further information.

(13) Huzinaga, S.; Miguel, B. *Chem. Phys. Lett* **1990**, *175*, 289. Huzinaga, S.; Klobukowski, M. *Chem. Phys. Lett* **1993**, *175*, 260.

(14) Gropen, O. *J. Comput. Chem.* **1987**, *8*, 983.

(15) Huzinaga, S.; Anzelm, J.; Klobukowski, M.; Radzio-Andzelm, E.; Sakai, Y.; Tatewaki, H. *Gaussian Basis Sets for Molecular Calculations*; Elsevier: Amsterdam, 1984.

(16) Rassolov, V.; Pople, J. A.; Ritner, M.; Windus, T. L. *J. Chem. Phys.* **1989**, *109*, 1223.

(17) Jansen, G.; Hess, B. A. *Chem. Phys. Lett.* **1989**, *160*, 507.

(18) Bader, R. F. W. *Chem. Rev.* **1991**, *91*, 893−928.